

LINEAR POLARIZATION OF THE MOON AT 6, 11, AND 21 CM WAVELENGTHS

By R. D. DAVIES*† and F. F. GARDNER*

[*Manuscript received July 20, 1966*]

Summary

The 210 ft radio telescope at Parkes provides adequate resolution at wavelengths of 6, 11, and 21 cm for the derivation of the distribution of linear polarization across the disk of the Moon. The polarization observations indicate an increase in dielectric constant with increasing wavelength.

The observed brightness distributions at all wavelengths indicate a rough surface. A roughness corresponding to a mean tilt of surface normals of about 12° is consistent with both the brightness and polarization distributions, and also with 68 cm radar observations, which sample a similar depth of lunar material.

The dielectric constant of the rough surface model at 6 and 11 cm wavelengths is significantly less than that deduced from the radar data. The discrepancy may be removed in a model where the surface layer is composed of a mixture of materials of different dielectric constants. For example, a mixture of 65% $\epsilon = 1.6$ and 35% $\epsilon = 5.0$ would give the observed polarization characteristics at 11 cm and the radar reflectivity at 68 cm.

I. INTRODUCTION

Troitsky (1954) first pointed out the possibility of deriving information about the dielectric constant and roughness of the lunar surface from measurements of linear polarization. The method is based on the polarization dependence of reflection at a surface. The situation is illustrated in Figure 1 for an idealized narrow-beam antenna directed at a point P on the Moon. The antenna temperature T_a is given by

$$T_a = T_s R + T_M(1-R), \quad (1)$$

where T_s is the sky brightness temperature in the direction concerned, T_M is the temperature of the Moon's surface, assumed constant, and $R(\theta)$ is the power reflection coefficient at incidence angle θ .

R has its extreme values when the electric field vector is parallel to (R_{\parallel}) and perpendicular to (R_{\perp}) the plane of incidence EPX. The Moon's contribution then gives rise to a polarization temperature (maximum–minimum) of $T_M(R_{\perp} - R_{\parallel})$ with the maximum electric field in the plane of incidence, whereas that of the sky background $T_s(R_{\parallel} - R_{\perp})$ has a minimum under this condition. Because T_s increases with decreasing frequency, approximately as $f^{-2.6}$, there will be some frequency in the vicinity of 150 Mc/s at which the net polarization will be zero. At frequencies of 1000 Mc/s and above only the Moon's contribution is significant, and the mean

* Division of Radiophysics, CSIRO, University Grounds, Chippendale, N.S.W.

† On leave from Nuffield Radio Astronomy Laboratories, Jodrell Bank, England.

brightness temperature T_b and the degree of polarization m are given by

$$T_b = T_M \{1 - \frac{1}{2}(R_{\parallel} + R_{\perp})\} \quad (2)$$

and

$$m = \frac{1}{2}(R_{\perp} - R_{\parallel}) / \{1 - \frac{1}{2}(R_{\parallel} + R_{\perp})\}. \quad (3)$$

For a smooth surface and lunar material with a dielectric constant ϵ and zero conductivity, the power reflection coefficients are the square of the usual Fresnel coefficients, namely

$$R_{\parallel}(\theta) = \left| \frac{\epsilon \cos \theta - (\epsilon - \sin^2 \theta)^{\frac{1}{2}}}{\epsilon \cos \theta + (\epsilon - \sin^2 \theta)^{\frac{1}{2}}} \right|^2 \quad (4)$$

and

$$R_{\perp}(\theta) = \left| \frac{\cos \theta - (\epsilon - \sin^2 \theta)^{\frac{1}{2}}}{\cos \theta + (\epsilon - \sin^2 \theta)^{\frac{1}{2}}} \right|^2. \quad (5)$$

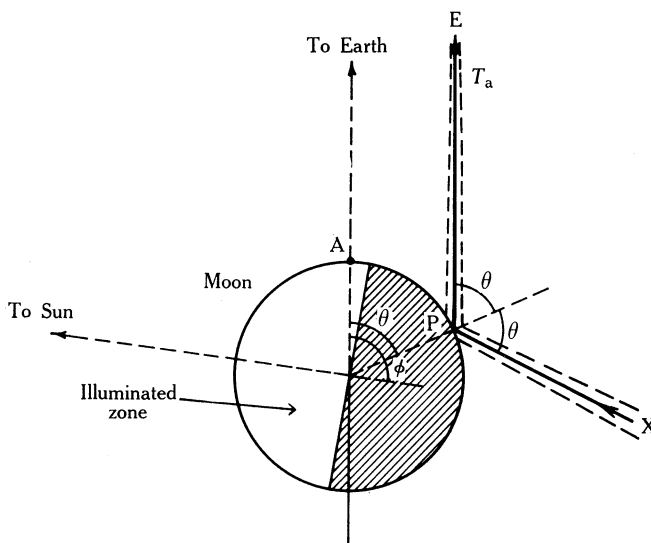


Fig. 1.—Illustration of the observation of a lunar point P, situated in the plane defined by the centres of the Moon, Earth, and Sun, with an idealized antenna whose beamwidth is much narrower than the Moon.

The idealized situation is complicated by the effects of roughness and by changes in the Moon's composition and temperature with depth. The subject has been discussed in detail in a recent review by Troitsky (1965). The actual observations are further affected by the finite beam size of the antenna and by departures from circular symmetry.

Polarization observations made by Soboleva (1962) at 3.2 cm, by Heiles and Drake (1963) at 21 cm, by Golnev and Soboleva (1964) at 6.3 cm, and by Baars *et al.* (1965) at 2.1 cm have indicated dielectric constants in the range 1.6–2.1.

Additional information on the lunar surface has been derived from the distribution of brightness across the disk (Troitsky 1962), and from radar measurements of reflectivity (Evans and Pettengill 1963; Muhleman 1964) and of depolarization

(Hagfors *et al.* 1965). The radar reflectivity indicates a dielectric constant in the range 2.6–2.8, considerably higher than the value obtained from polarization and brightness measurements. Attempts have been made to resolve the discrepancy by Hagfors and Morriello (1965) and others by introducing surface roughness. We consider some models in Section V.

The present observations of polarization and brightness temperature distributions at 6, 11, and 21 cm wavelengths, made with the Parkes 210 ft dish, were intended to give more detailed information on its wavelength dependence in the centimetre–decimetre band.

II. OBSERVATIONS

The particulars of the observational program are given in Table 1. Each set of observations consisted of scans in right ascension and declination through the centre of the Moon for the intensity distributions, plus polarization observations at a number of points along the two tracks.

TABLE 1
PARTICULARS OF OBSERVATIONS

Date (1963)	Type of Observation	Wavelength (cm)	Half-power Beamwidth	Moon Semidiam.	Age of Moon (days)	Position Angle of Rotation Axis
Oct. 30.5	Intensity and polarization	6	4'.4	16'.5	13.0	336°
May 13.7	Intensity	11.3	7.3	15.2	18.7	351
July 16.8	Intensity and polarization	11.3	7.3	16.2	25.4	350
Oct. 14.8	Intensity	11.3	7.3	15.0	26.9	24
May 29.8	Intensity	21.4	14.4	15.3	6.2	21
July 30.6	Intensity and polarization	21.4	14.4	14.8	9.6	16

III. POLARIZATION MEASUREMENTS AND SOURCES OF ERROR

The basic method consisted of measuring the change of intensity with rotation of a linearly polarized feed system, as the telescope tracked firstly a chosen point on the Moon and secondly a comparison region of sky. A sine wave with an angular period of 180° was fitted to the difference between the “on-source” and “off-source” rotations. Errors in polarization measurements with the Parkes telescope, which has an altazimuth mount, have been discussed by Gardner and Davies (1966) in connection with measurements on sources of small angular diameter. Because the aerial temperature from the Moon is high, galactic polarization effects are negligible, but *gain* and beam “*ellipticity*” effects are important. In addition, uncertainty in the position of the telescope beam relative to the centre of the Moon, of about ± 1 min of arc, during a series of observations lasting up to 2 hr is responsible for some scatter in the polarization values, particularly for points near the limb of the Moon, where their intensity is most sensitive to small changes in pointing.

(a) Gain Variation with Angle of the Feed

The variation of the antenna gain with feed angle gives rise to an apparent polarization, as discussed by Gardner and Davies (1966). The basic checks were made with the beam centred on the unpolarized* small diameter sources, Orion A and Hydra A. These showed an apparent polarization of about $1.6(\pm 0.4)\%$ at 6 cm, $1.3(\pm 0.3)\%$ at 11 cm, and less than 0.3% at 21 cm. In all cases the instrumental polarization gave maximum intensity at one particular feed angle.

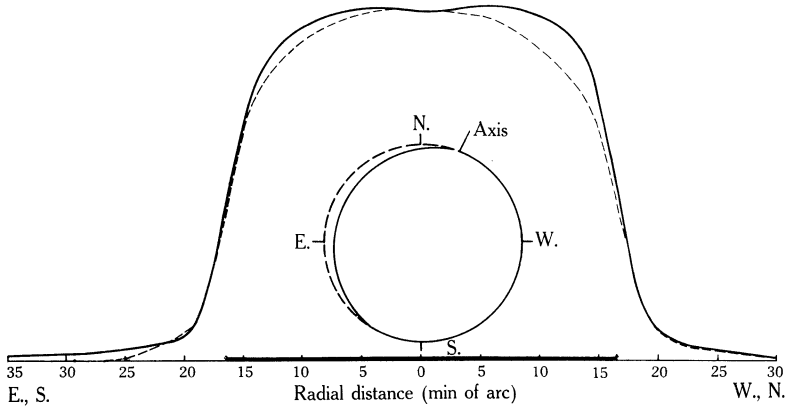


Fig. 2.—6 cm observed brightness distributions for October 30.5, 1963; — R.A. scan, - - - Dec. scan. The illuminated portion of the Moon is enclosed by solid arcs.

(b) Beam Ellipticity

This was determined from polarization observations at a series of antenna-beam offsets from the centres of Orion A and Hydra A. It is necessary to convolve the distribution of apparent polarization with an intensity distribution similar in form to the edge of the Moon to obtain the overall corrections. For a uniform disk the spurious polarization is zero at the limb and changes in angle by 90° from outside to inside the limb. The maximum values of polarization derived were under 0.2% at 6 and 21 cm and about 0.3% at 11 cm, expressed as a percentage of the Moon's central intensity.

A more direct check was made at 11 and 21 cm using the extended galactic sources IC 443 and W 44, which have diameters of $\sim 0.5^\circ$ and sharp circular edges in at least one quadrant. The polarization at the edge of these extended sources was measured to be less than 0.5% at both 11 and 21 cm, while the angle was approximately that expected from the beam ellipticity in each case. This result is consistent with that derived from the convolution process assuming that there is no true polarization in the two sources.

* $< 0.3\%$ at 20 cm and 11 cm (Gardner and Davies 1966) and $< 0.4\%$ at 6 cm (unpublished Parkes observations).

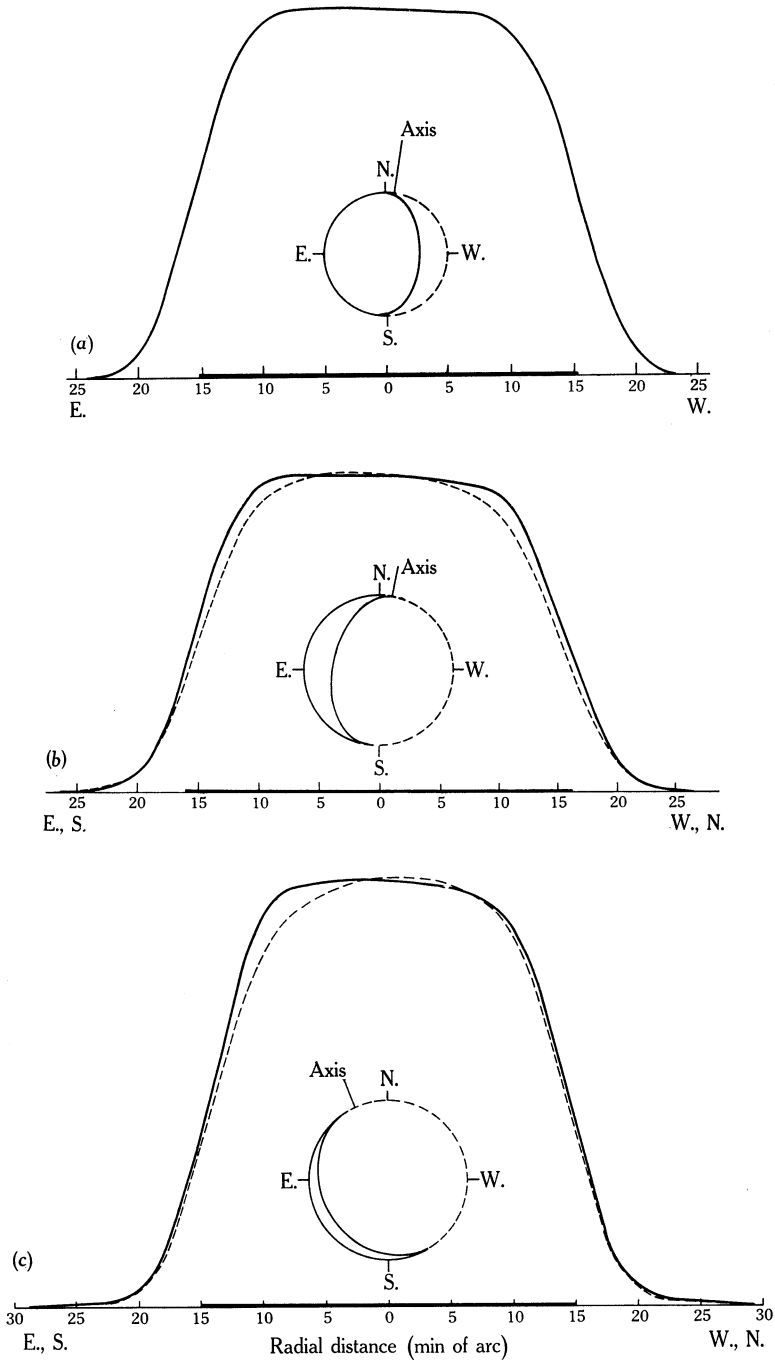


Fig. 3.—11 cm observed brightness distributions for (a) May 13·7, (b) July 16·8, and (c) October 14·8, 1963; — R.A. scan, - - - Dec. scan.

IV. INTENSITY DISTRIBUTIONS

(a) *Observed Distributions*

The total intensity distributions are shown in Figures 2, 3, and 4 for 6, 11, and 21 cm respectively. For each set of right ascension (east-west) and declination (north-south) scans the illumination and the rotation axes of the Moon are shown. The intensities were corrected for non-linearity of the receivers, but absolute calibration of the temperature scale was not attempted. At 11 and 21 cm the curves shown are the mean of scans made with orthogonal polarizations, while at 6 cm the scans were made with one polarization and then adjusted for the polarization observed on the same day. The accuracy of the observations is limited only by the characteristics of the telescope beam and the accuracy of the telescope tracking (noise fluctuations are less than 0.3% of the peak intensity in each instance), which have been

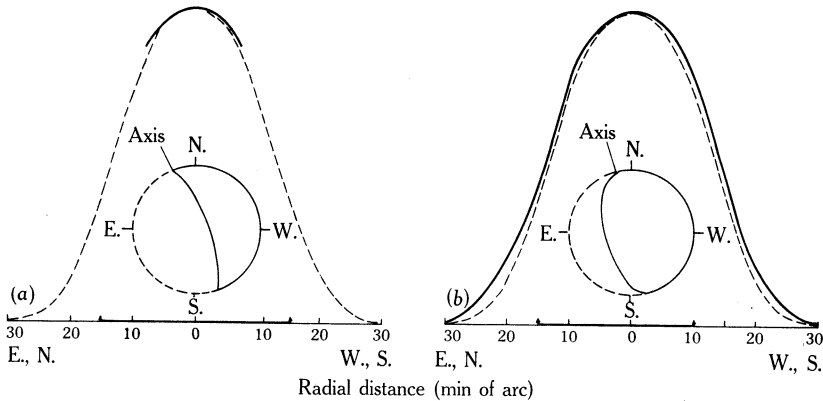


Fig. 4.—21 cm observed brightness distributions for (a) May 29.8 and (b) July 30.6, 1963; — R.A. scan, - - - Dec. scan.

considered in connection with the polarization determinations, where they are more important. At 20 and 11 cm, errors are estimated to be under 1% of the peak when scans with orthogonal polarizations are averaged. At 6 cm, scattered radiation from surface irregularities of the reflecting surface gives rise to a broad distribution of side lobes, some 1–2 degrees in extent, in the general direction of the main beam. This causes the gradual rise in intensity before the main beam intercepts the lunar disk (see Fig. 2). It is still considered that intensity variations of angular extent comparable with the 4' beamwidth are accurate to 1% of the peak.

Figures 2, 3, and 4 all show noticeable limb darkening in the poleward direction. In addition, there was a variation across the disk at 6 and 11 cm, and possibly a small effect at 21 cm. This is principally the phase effect and the limited data available on this are discussed in the Appendix. At 6 cm there are local irregularities in brightness, which result in a shallow minimum at the centre of the disk.

(b) *Interpretation of Intensity Distributions*

The average of the east-west and west-east scans were used as the mean equatorial distribution for comparison with the theoretical models. These are shown in Figures 5, 6, and 7 for 6, 11, and 21 cm respectively, together with the distributions

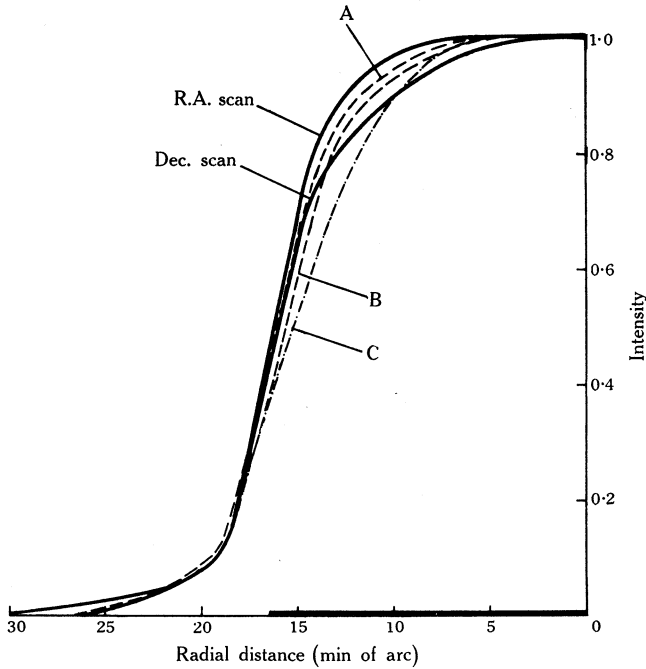


Fig. 5.—Mean 6 cm brightness distributions for October 30.5, 1963, compared with uniform brightness temperature (A), $\epsilon = 2.0$ (B), and $\cos^{1/2} \psi$ (C) models.

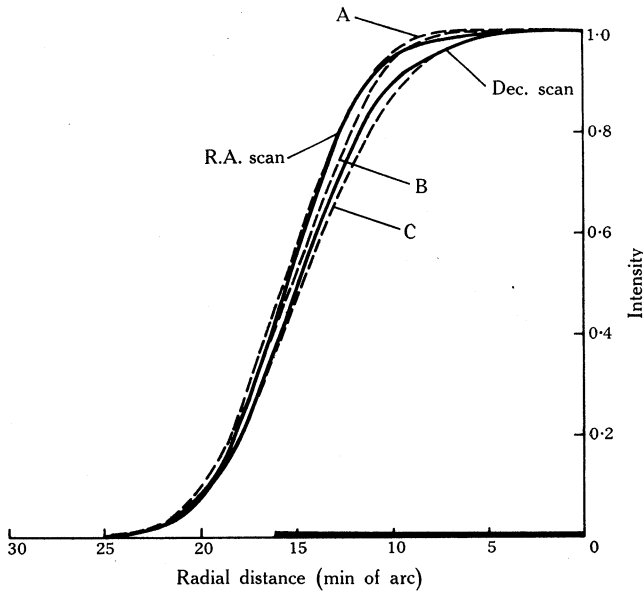


Fig. 6.—Mean 11 cm brightness distributions for July 16.8, 1963, compared with uniform brightness temperature (A), $\epsilon = 2.0$ (B), and $\cos^{1/2} \psi$ (C) models.

obtained by convolving the beam at each wavelength with two models: (A) one with uniform brightness temperature across the disk, and (B), for 6 and 11 cm only, one with a smooth surface dielectric constant $\epsilon = 2.0$ and constant T_M (equation (2)). In each case the distribution was normalized to unity at the centre of the disk.

At each wavelength the observed equatorial distribution is a better fit to the uniform brightness model. This gives an indication of the degree of surface roughness, which is considered in Section V. At 6 cm the distribution is slightly limb brightened—probably due to extended regions of local excess temperature.

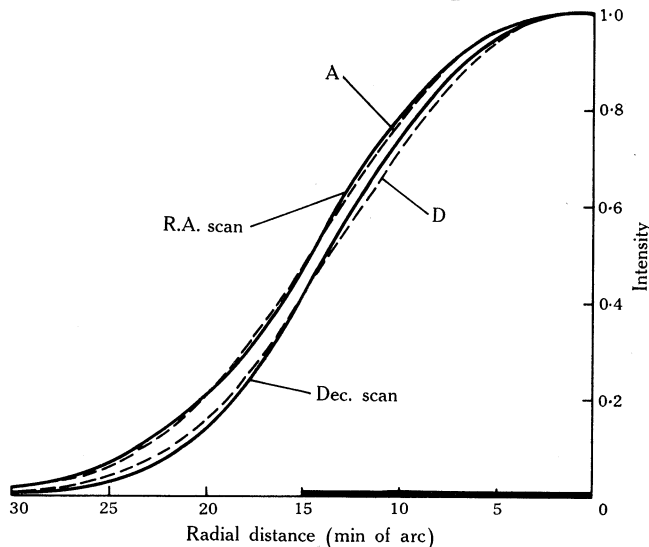


Fig. 7.—Mean 21 cm brightness distributions for July 30.6, 1963, compared with uniform brightness temperature (A) and $\cos^3 \psi$ (D) models.

Figures 5, 6, and 7 also contain the average of the north–south and south–north declination scans to give the mean distribution with latitude for comparison with a $\cos^3 \psi$ distribution (C) at 6 and 11 cm and with a $\cos^3 \psi$ distribution (D) at 20 cm, where ψ is the latitude. There appears to be a definite increase in the limb darkening at the longer wavelengths. At 6 cm the observed distribution is in reasonable agreement with the $\epsilon = 2.0$ distribution and is more uniform than the $\cos^3 \psi$ distribution; the 11 cm data correspond more closely to the $\cos^3 \psi$ than to the $\epsilon = 2.0$ distribution; at 21 cm the observed distribution is close to a $\cos^3 \psi$ variation.

V. POLARIZATION DISTRIBUTIONS

(a) Observational Results

At all points where significant polarization was detected the electric field was radial to within the errors of measurement, which were generally under 5° . The distribution of polarized intensity, expressed as a percentage of the central intensity, is shown in Figures 8–10. To correct for limb darkening, the polarized intensity at each declination point at 6 and 11 cm has been increased to the value expected if the brightness temperature were the same as at the corresponding right ascension point.

(b) *Interpretation of Polarization*

Figures 8, 9, and 10 also contain the polarization distributions calculated for the smooth-Moon case, from a convolution of the radial variation of the degree of polarization* (equation (3)) with the beam shape at the three wavelengths. The best fit of the observations is for dielectric constants of 2.00 ± 0.05 , 2.05 ± 0.05 , and 2.30 ± 0.15 at 6, 11, and 21 cm respectively.

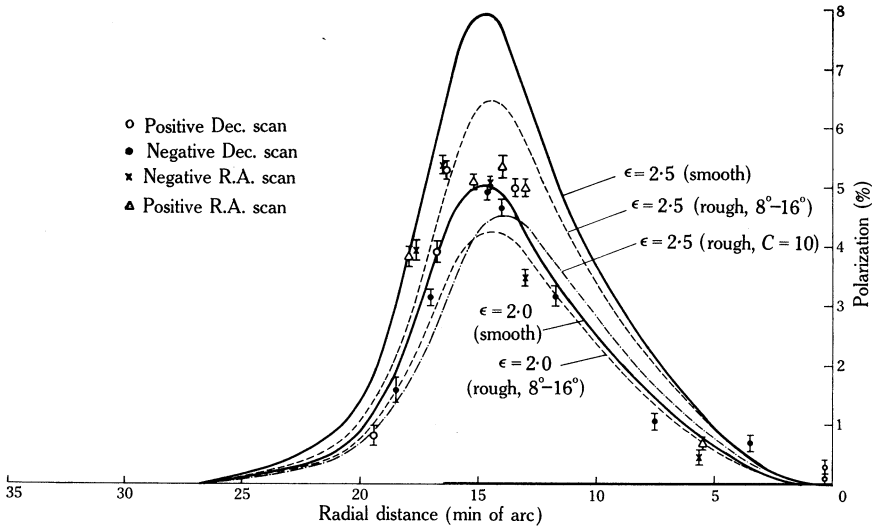


Fig. 8.—6 cm polarization observations of October 30.5, 1963. Expected distributions for $\epsilon = 2.0$ and 2.5 calculated for smooth and rough surfaces are also shown.

(c) *Effects of Roughness*

In order to assess the effect of surface roughness on polarization, calculations have been made for two simplified models on the lines of those proposed to explain radar observations.

From an analysis of radar reflectivity data at 68 cm Rea, Hetherington, and Mifflin (1964) have derived a distribution of slopes on the lunar surface. They find a mean tilt of the surface normal of 10–16 degrees and an r.m.s. value of 13–22 degrees. The surface roughness deduced from radar varies with wavelength, due to the increasing depths of penetration at longer wavelengths. Hagfors and Morriello (1965) consider that the same lunar depths will be responsible for emission at wavelengths λ_e and radar reflection at wavelength λ_r . For $\epsilon = 2.0$, $\lambda_r = 2\lambda_e$ at normal incidence and $\lambda_r = 5\lambda_e$ at grazing incidence. On this basis we might expect that the roughness derived from the quasi-specular component of the 68 cm radar results

* This procedure is based on the uniform brightness distribution of Section IV. Strictly speaking, the distribution of polarized intensity $T_M(R_\perp - R_\parallel)$ should be used in the convolution. This has a greater degree of polarized limb brightening between 15' and 17' of the Moon's centre, but with the beamwidths used in this investigation the difference in the two convolved distributions is small.

would provide a reasonable model for comparison with the polarization results. Accordingly, a simplified model was taken with wave normals distributed uniformly in the range 8–16 degrees. The mean and r.m.s. values of the model are consistent with the radar values. The calculated polarization distributions are shown in Figures 8, 9, and 10 for $\epsilon = 2.0$ and 2.5.

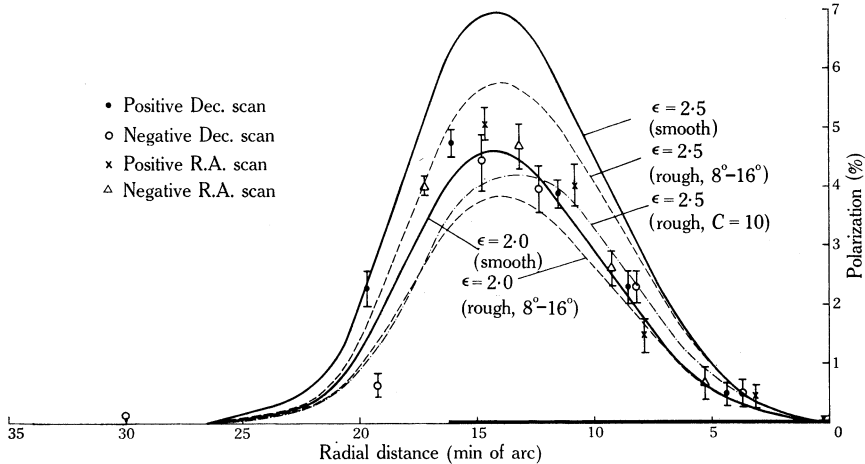


Fig. 9.—11 cm polarization observations of July 16.8, 1963. Expected distributions for $\epsilon = 2.0$ and 2.5 calculated for smooth and rough surfaces are also shown.

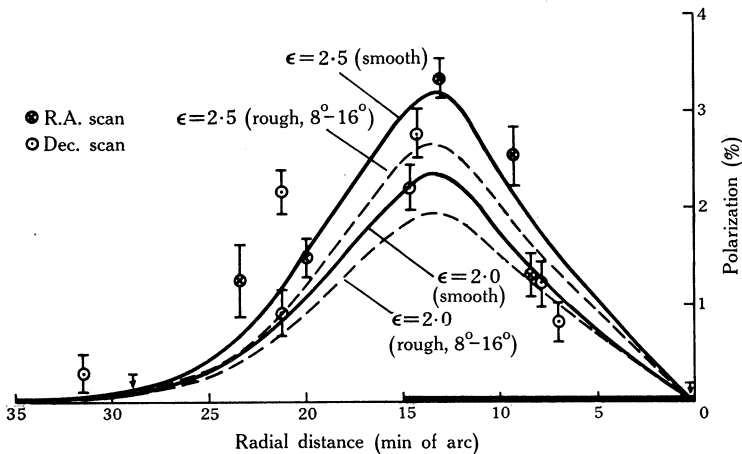


Fig. 10.—21 cm polarization observations of July 30.6, 1963. Expected distributions for $\epsilon = 2.0$ and 2.5 calculated for smooth and rough surfaces are also shown.

Alternative specifications of roughness, defined in terms of the statistical properties of the surface irregularities, have been investigated by Hagfors and Morriello. Their first "Gaussian" model with roughness parameter $S = 0.16$ is very similar in effect to the 8–16 degrees distribution of slopes, as is their second "exponential" model with roughness parameter $C \sim 20$. Calculations were made for a model with greater roughness, $C = 10$, and these are shown in Figures 8 and 9.

The best fit to the 6 cm observations with the 8–16 degrees slope model occurs for $\epsilon = 2.2 \pm 0.1$. The fit is *not as good* as with the smooth model for $\epsilon = 2.0$. The rougher model $C = 10$ is incompatible with the data. At 11 and 21 cm the fit with the rough model is no better than with the smooth; the corresponding best fitting values of ϵ are 2.25 ± 0.05 and 2.50 ± 0.15 . Again at 11 cm the rougher model $C = 10$ does not fit the data.

A further argument relating to the roughness comes from the equatorial brightness distributions, where the 6 and 11 cm distributions can *only* be fitted with a model having roughness at least as great as the 8–16 degrees adopted. Thus to sum up, the combined brightness and polarization data at 6, 11, and 21 cm indicate a roughness represented by an 8–16 degrees scatter angle, corresponding to a Gaussian autocorrelation function with $S = 0.16$ or an exponential function with $C = 20$.

TABLE 2

DIELECTRIC CONSTANTS DERIVED FROM POLARIZATION OBSERVATIONS AT VARIOUS WAVELENGTHS

Wavelength (cm)	Smooth Model ϵ	Rough Model ϵ Scatter		Observers
2.1	1.8 ($R = 0.0-0.6$)	1.5 ($R = 0.6-0.9$)	$\pm 15^\circ$ cone	Baars <i>et al.</i> (1965)
3.2	1.55*	1.65	$\pm 20^\circ$ cone	Soboleva (1962)
6.3	1.9*	2.0*	$\pm 20^\circ$ cone	Golnev and Soboleva (1964)
6	2.00 ± 0.05	2.2 ± 0.1	$8^\circ-16^\circ$	Present work
11	2.05 ± 0.05	2.25 ± 0.05	$8^\circ-16^\circ$	Present work
21	2.3 ± 0.15	2.50 ± 0.15	$8^\circ-16^\circ$	Present work
21	2.1 ± 0.3	—	—	Heiles and Drake (1963)

* Estimated from the published data of observers.

VI. DISCUSSION OF RESULTS

Published polarization results, including those from the present experiment, are summarized in Table 2. The increase in dielectric constant with wavelength appears to be established whether the data are interpreted in terms of smooth or rough models. Because the radio wave penetration increases with wavelength, the measured dielectric constants at the longer wavelengths refer to greater depths beneath the surface and the dielectric-constant increase is presumably a consequence of the lunar material at greater depths being more closely packed. The depth of emission may be specified using the data presented by Troitsky (1962, 1965) for a model based on terrestrial silicate rocks. The thickness of the radiating layer ≈ 20 wavelengths (equation (19) of Troitsky 1962), while the density ρ and dielectric constant are related by $\epsilon^{\frac{1}{2}} - 1 = 0.5\rho$ (equation (5) of Troitsky 1965). With these formulae the dielectric constant of 1.5 found at 2.1 cm wavelength would indicate a density of 0.5 g/cm^3 at a depth of around 40 cm, while a dielectric constant of 2.3 at 21 cm wavelength would indicate a density of 1.0 g/cm^3 at about 4 m.

The roughness deduced from polarization and brightness data appears to be of the same magnitude in the wavelength range 2.1–11 cm (the 21 cm results are not

accurate enough to determine a value of the roughness). This indicates that at the depths of emission at each wavelength the emitting surfaces, which are at least several wavelengths across, are distributed with surface normals lying at similar scattering angles. A terrain on which large relatively dense boulders forming a sub-surface layer are overlaid with less dense fragments forming a low density surface layer is compatible with the data. The existence of a more tenuous layer at the surface has also been demonstrated by the radar depolarization measurements of Hagfors *et al.* (1966).

The polarization measurements, even with allowance for roughness, give dielectric-constant values significantly below the 2.8 from radar data. One way of accounting for this difference is to postulate that the lunar material consists of a mixture of dielectric constants. An addition of a fraction of higher dielectric constant causes a greater increase in reflectivity than in polarization. As an example, the observed polarization results at 11 cm and the radar reflectivity would be produced by a mixture comprising 65% with $\epsilon = 1.6$ and 35% with $\epsilon = 5.0$, a typical value for terrestrial rocks. The observed increase in polarization with increasing wavelength could be explained in terms of an increase in the proportion of higher dielectric-constant material at greater depths.

The present study of the latitude brightness distribution at 6, 11, and 21 cm shows a trend towards a more uniform illumination at the shorter wavelengths. The distribution changes from a $\cos^3 \psi$ law at 21 cm to a distribution that is nearly uniform with $\epsilon = 2.0$ at 6 cm or at the limits of the errors of measurement a $\cos^3 \psi$ law. This trend appears to extend to the infrared, where at 8.8μ the latitude distribution is close to uniform (Geoffrion, Korner, and Sinton 1961). However, the wavelength variations are more obscure in the short centimetre and millimetre wave region where a $\cos^3 \psi$ variation has been reported (Krotikov and Troitsky 1962; Salomonovich 1962). These observations do not appear to have taken polarization into account; also they are at wavelengths where the phase effect is large and this makes the separation of the latitude variation more difficult.

VII. REFERENCES

- BAARS, J. W. M., MEZGER, P. G., SAVIN, N., and WENDKER, H. (1965).—*Astr. J.* **70**, 132.
 EVANS, J. V., and PETTENGILL, G. H. (1963).—*J. geophys. Res.* **68**, 423.
 GARDNER, F. F., and DAVIES, R. D. (1966).—*Aust. J. Phys.* **19**, 441.
 GEOFFRION, A. R., KORNER, M., and SINTON, W. M. (1961).—*Bull. Lowell Obs.* **5**, 1.
 GOLNEV, V. J., and SOBOLEVA, N. S. (1964).—*Proc. astr. Obs. Pulkova* **13**, 83.
 HAGFORS, T., BROCKELMAN, R. A., DANFORTH, H. H., HANSON, L. B., and HYDE, G. M. (1965).—*Science* **150**, 1153.
 HAGFORS, T., and MORRIELLO, J. E. (1965).—*J. Res. natn. Bur. Stand.* **69D**, 1614.
 HEILES, G. E., and DRAKE, F. D. (1963).—*Icarus* **2**, 281.
 KISLYAKOV, A. G. (1962).—Symp. IAU No. 14.
 KROTIKOV, V. D., and TROITSKY, V. S. (1962).—*Astr. Zh.* **39**, 1089.
 MUHLEMAN, D. O. (1964).—*Astr. J.* **69**, 34.
 REA, D. G., HETHERINGTON, N., and MIFFLIN, R. (1964).—*J. geophys. Res.* **69**, 5217.
 SALOMONOVICH, A. E. (1962).—*Astr. Zh.* **39**, 79.
 SOBOLEVA, N. S. (1962).—*Astr. Zh.* **39**, 1124.
 TROITSKY, V. S. (1954).—*Astr. Zh.* **31**, 511.
 TROITSKY, V. S. (1962).—Symp. IAU No. 14.
 TROITSKY, V. S. (1965).—*Radio Sci.* **69**, 1585.

APPENDIX

Some Observations of the Phase Effect on the Moon at 6, 11, and 21 cm Wavelengths

With the resolution of the telescope it is possible to derive some information on the phase variation during a lunation from the distribution of temperature across the disk under partial illumination. As drawn in Figure 1 the Moon's centre A is at

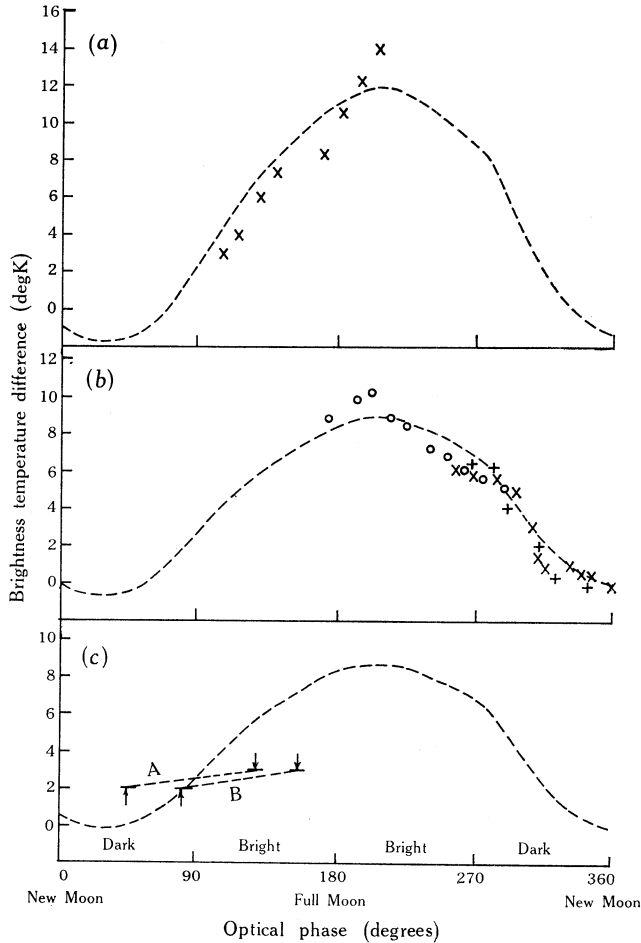


Fig. 11.—Observations of phase variation of brightness temperature for the centre of the lunar disk at (a) 6 cm for October 30.5; (b) 11 cm for October 14.8 (+), May 13.9 (O), and July 16.8 (x); and (c) 21 cm for May 29.8 (A) and July 30.6 (B). The central brightness temperature was $\sim 220^\circ\text{K}$ in each case. The shape of the 0.4 cm (Kislyakov 1962) variation is shown at each wavelength for comparison.

phase ϕ , while point P is at phase $(\phi - \theta)$. For θ less than about 45° the aerial temperature in the direction of P will approximate the central temperature at the earlier phase $(\phi - \theta)$, since the emissivity does not change rapidly with θ in this range. With this assumption the right ascension scans were used to derive the phase variations

shown in Figure 11, where they are compared with the variation found at 4 mm by Kislyakov (1962), which is plotted on an arbitrary scale in the figure. The form of the phase variation at wavelengths at least up to 3.2 cm is similar (Salomonovich 1962). The present 11 cm data fit this shape and indicate a temperature variation over a lunation of 9 degK. If both the 6 and 21 cm data were to fit a variation of the same shape, the maximum temperature variation in each case would be 15-20 and ≤ 3 degK respectively. The decreasing amplitude of the phase effect at increasing wavelengths indicates that the longer wavelength radiation comes from deeper within the lunar surface where the amplitude of the thermal wave is smaller.